Journal of Optics A: Pure and Applied Optics

A reliable phase unwrapping algorithm based on the local fitting plane and quality map

To cite this article: Yongjian Zhu *et al* 2006 *J. Opt. A: Pure Appl. Opt.* **8** 518

INSTITUTE OF PHYSICS PUBLISHING JOURNAL OF OPTICS A: PURE AND APPLIED OPTICS

J. Opt. A: Pure Appl. Opt. **8** (2006) 518–523 doi:10.1088/1464-4258/8/6/005

A reliable phase unwrapping algorithm based on the local fitting plane and quality map

Yongjian Zhu[1], **Liren Liu, Zhu Luan and Anhu Li**

Shanghai Institute of Optics and Fine Mechanics, Chinese Academy of Sciences, PO Box 800-211, Shanghai 201800, People's Republic of China

E-mail: zhuyongjian_siom@yahoo.com.cn

Received 4 January 2006, accepted for publication 12 April 2006
Published 28 April 2006
Online at stacks.iop.org/JOptA/8/518

Abstract
A fast and reliable phase unwrapping (PhU) algorithm, based on the local quality-guided fitting plane, is presented. Its framework depends on the basic plane-approximated assumption for phase values of local pixels and on the phase derivative variance (PDV) quality map. Compared with other existing popular unwrapping algorithms, the proposed algorithm demonstrated improved robustness and immunity to strong noise and high phase variations, given that the plane assumption for local phase is reasonably satisfied. Its effectiveness is demonstrated by computer-simulated and experimental results.

Keywords: phase unwrapping, fitting plane, quality map, cost function

1. Introduction

In many two-dimensional signal processing applications, an important problem is the unwrapping of two-dimensional phase functions. For example, in interferometric synthetic aperture radar (IFSAR) or three-dimensional profilometry [1] applications, in order to reconstruct a continuous phase field, one should perform the phase unwrapping (PhU) [2] operation to remove the existing phase ambiguities. The PhU denotes the retrieval of the original (unwrapped) phase ϕ from the corresponding restricted (wrapped) phase φ in the $(-\pi, \pi)$ interval. The unwrapped process seems simple in principle, but it will lead to unreliable phase results and make the recovery of a true phase field challenging if the wrapped-phase map contains such defects as strong noise [3] and inconsistencies.

For over two decades many PhU algorithms have been proposed to improve the reliability of the unwrapped-phase results. These algorithms can be grouped into three classes [4]: (1) global algorithms, (2) region algorithms, and (3) path-following algorithms.

The global algorithms formulate the unwrapping algorithm in terms of minimization of a global function [5]. All the algorithms in this class are known to be robust but computationally intensive [4, 6, 7]. The region algorithms [8–10] divide the full image into sub-parts to successively recombine them once they have been unwrapped. The region algorithms provide a compromise between the robustness and the computational intensity [8]. The path-following algorithms [7, 11–14] perform phase integration in a sequence of steps to recover the true phase field. They can be subclassified into three groups [4]: (1) path-dependent algorithms, (2) residue-compensation algorithms, and (3) quality-guided path algorithms. These path-dependent algorithms such as Goldstein's branch cuts [11] and mask cuts [13] are generally computationally efficient but not robust [6].

In addition to the above algorithms, in 1995, Hock Lim was the first to propose a plane-fitting unwrapping algorithm. The phase-unwrapping process begins at a location where the phase pattern is relatively flat, thus enabling confident determination of the phase values of the local pixels [15]. In general, it has been found to be capable of reasonably unwrapping IFSAR interferograms. However, this method performs the unwrapping operation only along the direction of the plane's gradient, which may fail to correctly unwrap when encountering rapid phase changes. At the same time, because it has not introduced the quality information and taken the effect

[1] Author to whom any correspondence should be addressed.

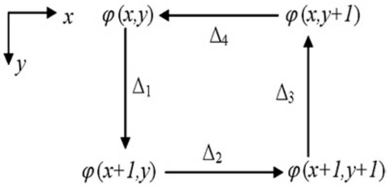

Figure 1. The four neighbour pixels of a wrapped phase.

of residues [7] into account, this method has not shown ideal noise robustness in the presence of strong noise. So we here modify the plane-fitting PhU algorithm in a simplified and efficient way, and improve it by considering the residues and introducing quality information into the unwrapping process. Then we provide a simulated phase map with strong noise and an IFSAR map with high phase variations to verify the noise robustness and reliability of the proposed scheme.

In this paper, section 2 describes the principle of the proposed plane-fitting PhU algorithm; sections 3 and 4 present the numerical and experimental data, respectively, to test the proposed algorithm, and compare our algorithm with some conventional path-following algorithms; finally, section 5 summarizes our conclusions.

2. Principle

2.1. PhU problem

The relationship between the wrapped phase $\varphi(x, y)$ and the unwrapped phase $\phi(x, y)$ may be stated as

$$\varphi(x, y) = W[\phi(x, y)] = \mathrm{mod}\{[\pi + \phi(x, y)], 2\pi\} - \pi, \quad (1)$$

$$-\pi < \varphi(x, y) < \pi, \quad (2)$$

where W is the wrapping operator. The PhU means to retrieve the continuous unwrapped-phase values from the wrapped map. According to Itoh's description [2], one can solve the PhU problem by integrating the wrapped values of the differences of the wrapped phase. But in fact, due to the presence of residues and noise, it becomes very difficult to perform the PhU operation. So to obtain a better true phase field, one can remove the noise pixels and residues [7] as much as possible.

Figure 1 shows the four neighbouring pixels in the grid of a wrapped phase, and where each wrapped-phase value is divided by 2π.

One can identify the residues by the equation

$$\begin{aligned} q = \sum_{i=1}^{4} \Delta_i &= [\varphi(x, y+1) - \varphi(x, y)] + [\varphi(x+1, y+1) \\ &- \varphi(x, y+1)] + [\varphi(x+1, y) - \varphi(x+1, y+1)] \\ &+ [\varphi(x, y) - \varphi(x+1, y)], \end{aligned} \quad (3)$$

where, when $q = 0$, there is no residue; when $q = -1$, the residue (x, y) is negative and otherwise, $q = 1$ represents the positive charge. One may use a median filter or averaging filter to remove the residues.

2.2. Quality-guided plane-fitting PhU algorithm

A quality map is a two-dimensional data array which can measure the quality or goodness of each pixel from the wrapped-phase map. In quality map, the areas with low quality represent unreliable phase data.

There exist four conventional quality maps: correlation, pseudo-correlation (PSD), phase derivative variance (PDV) and maximum phase gradient (MPG). The correlation map is the best, but it is not derivable from the phase data alone. In one's experience, the PDV seems to be the most useful map in practice. The MPG is also useful, although it sometimes yields poor results, and the PSD map is the least satisfactory of the four quality maps [7].

The PDV quality value at the pixel (x, y) is defined as

$$q(x, y) = \frac{\sqrt{\sum_{i=x-k/2}^{x+k/2} \sum_{j=y-k/2}^{y+k/2} (\Delta_{i,j}^{x} - \bar{\Delta}_{x,y}^{x})^2} + \sqrt{\sum_{i=x-k/2}^{x+k/2} \sum_{j=y-k/2}^{y+k/2} (\Delta_{i,j}^{y} - \bar{\Delta}_{x,y}^{y})^2}}{k \times k}, \quad (4)$$

where k is the window size with the centre pixel (x, y),

$$\Delta_{i,j}^{x} = W\{\varphi(i+1, j) - \varphi(i, j)\}, \quad (5)$$

$$\Delta_{i,j}^{y} = W\{\varphi(i, j+1) - \varphi(i, j)\}, \quad (6)$$

the terms $\Delta_{i,j}^{x}$ and $\Delta_{i,j}^{y}$ are the partial derivatives of the phase. The terms $\bar{\Delta}_{x,y}^{x}$ and $\bar{\Delta}_{x,y}^{y}$ are the averages of these partial derivatives in the $k \times k$ windows. In application, the PDV quality values are assumed to be negated to measure the goodness of phase data. We will introduce the PDV quality information into the plane-fitting PhU algorithm.

From [15, 16], we know the plane-fitting PhU algorithm is based on the assumption that the unwrapped-phase values of the pixels in a 3×3 window may be closely approximated locally by a plane, so we define the plane with the equation

$$\phi_{\mathrm{e}}(x, y, \alpha, \beta) = c(x, y) + s_x(x, y)(\alpha - x) + s_y(x, y)(\beta - y), \quad (7)$$

where (α, β) are the coordinates of a pixel in the 3×3 window with the centre pixel (x, y); $c(x, y)$ is the intercept of phase plane at the pixel (x, y); $s_x(x, y)$ and $s_y(x, y)$ are the slopes of the tangents along the x and y directions, respectively. Let $\phi(\alpha, \beta)$ be the unwrapped-phase values of the pixels in the 3×3 window, and $U_{x,y}(c, s_x, s_y)$ be the mean-square cost function [17],

$$U_{x,y}(c, s_x, s_y) = \sum_{(\alpha,\beta)\in N_{x,y}} [\phi(\alpha, \beta) - \phi_{\mathrm{e}}(x, y, \alpha, \beta)]^2, \quad (8)$$

where the term $N_{x,y}$ is the 3×3 window with the centre pixel (x, y); $\phi(\alpha, \beta)$ chooses a value from the following equations:

$$\phi(\alpha, \beta) = \varphi(\alpha, \beta) \pm 2k\pi, \quad (9)$$

where $\varphi(\alpha, \beta)$ is the wrapped-phase value. The term k is a positive integer which lets $\phi(\alpha, \beta)$ satisfy the following inequality:

$$-\pi < \phi(\alpha, \beta) - \phi_{\mathrm{e}}(x, y, \alpha, \beta) < \pi. \quad (10)$$

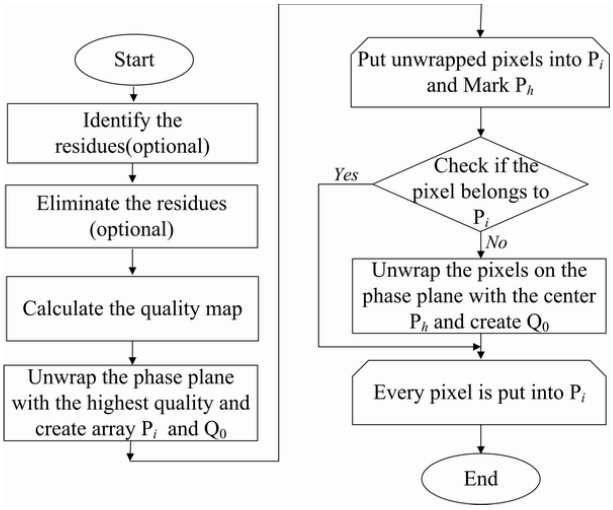

Figure 2. The flow chart of the proposed algorithm.

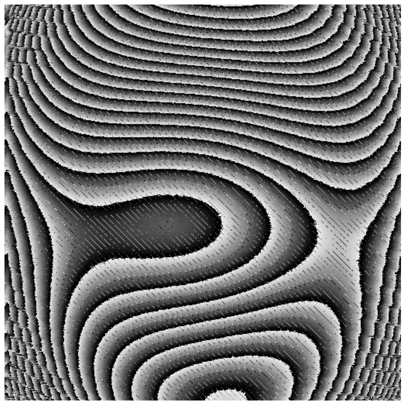

Figure 3. The simulated wrapped-phase map with strong noise and blurred background (512 × 512 pixels).

Figure 4. The PDV quality map of figure 3 (black means low in phase quality).

Therefore, from equation (8), one can first obtain the values of the parameters such as $c(x, y)$, $s_x(x, y)$ and $s_y(x, y)$ by minimizing the value of $U_{x,y}(c, s_x, s_y)$; then, choose a proper value of k to satisfy the inequality (10); and finally, extract the unwrapped-phase value $\phi(\alpha, \beta)$ from equations (9). In this way, the 3×3 pixels are unwrapped at one time. Moreover, one can speed up the process by unwrapping some different phase areas simultaneously. This description of the plane-fitting method makes the PhU simple and easy to program. It provides a fast and efficient way to unwrap the phase map without noise. But by only depending on the fitting plane, this method cannot show good noise robustness, and also it cannot solve the problem caused by sharp phase changes. Therefore, it is necessary to introduce the PDV quality information into this method. In this way, one can unwrap the reliable pixels first so as to avoid the above disadvantages and minimize the errors.

In the process of unwrapping, one can start the PhU on the highest-quality phase plane, and continue it under the guidance of the PDV quality information. The detailed steps are as follows:

(1) according to section 2.1, identify the residues (optional for a map without noise);
(2) remove the residues and noise by an averaging filter or median filter (optional for a map without noise);
(3) calculate the PDV quality values of the whole wrapped-phase map;
(4) start the PhU at the highest-quality pixel by use of the plane-fitting algorithm, calculate the values of the parameters c, s_x, s_y and k; put its 8-neighbouring pixels into a queue Q_0 and sort them by quality value;
(5) mark the unwrapped pixels and put them into an array P_i; select the highest-quality pixel P_h from Q_0, then unwrap the pixels on the fitting phase plane with the centre pixel P_h;
(6) create the queue Q_0 according to step (4); repeat step (5); unwrap all the pixels except those in the array P_i.

After step (6), all the pixels are unwrapped. Note that one can improve the efficiency by unwrapping many high-quality phase areas simultaneously for a large map. Figure 2 is the flow chart of the proposed algorithm.

We here provide numerical and experimental examples to test the validity of the proposed algorithm.

3. Numerical results

We test the proposed algorithm by use of a simulated wrapped-phase map which contains strong noise and blurred background. In the wrapped map, the wrapped phase is scaled so that black represents $-\pi$ rad and white represents π rad. Meanwhile, unwrapped-phase maps are also scaled between black and white to cover all the dynamic range. Figure 3 is a noisy simulated wrapped-phase map, which is 512×512 pixels in size and contains 8605 resides.

Figure 4 is the PDV quality map of figure 3.

The quality map (black means low in phase quality) with a lot of black speckles shows that the wrapped-phase map is polluted seriously by noise. Figure 5(d) is the phase map unwrapped by our algorithm.

For comparison, we also provide another three unwrapped-phase maps, as shown in figures 5(a)–(c). Figure 5(a) is the phase map unwrapped by Goldstein's branch cuts algorithm; figure 5(b) is the phase map unwrapped by the mask cuts algorithm with the PDV quality guidance; figure 5(c) is the phase

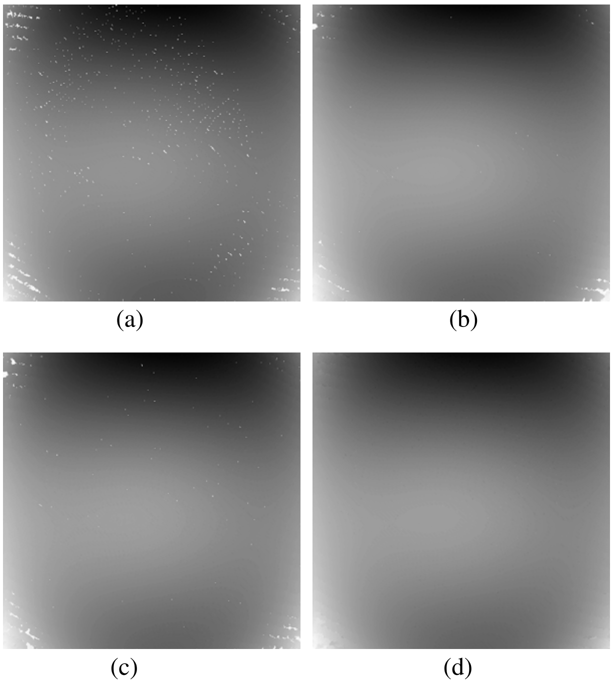

Figure 5. The unwrapped-phase map: (a) the phase map unwrapped by Goldstein's branch cuts algorithm; (b) the phase map unwrapped by the mask cuts algorithm; (c) the phase map unwrapped by the plane-fitting algorithm without quality guidance; (d) the phase map unwrapped by our proposed algorithm.

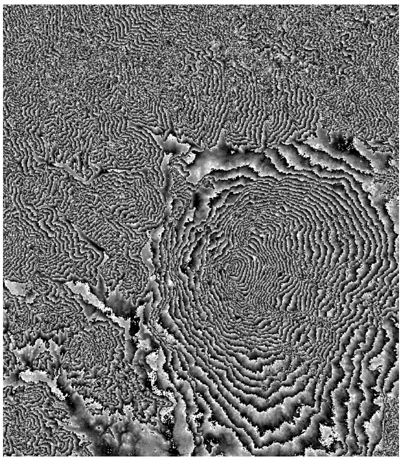

Figure 6. The wrapped-phase map obtained from the interferometry of a pair of SAR images of the Mount Etna volcano region, Sicily, Italy (grey level representation, 512 × 578 pixels).

map unwrapped by the plane-fitting algorithm without quality guidance. Figures 5(a)–(c) show that there are apparent unwrapped errors in the areas with white speckles. We compare figures 5(a)–(d) with the corresponding ideal unwrapped-phase surface without any noise present and calculate the root-mean-square (RMS) deviations, respectively. The RMS deviations of figures 5(a)–(d) are 1.954, 0.772, 0.921 and 0.286 rad, respectively. The data demonstrate that in dealing with the noisy phase map, our proposed algorithm could have higher reliability than the other three previously reported algorithms.

Figure 7. The PDV quality map of figure 6 (black means low in phase quality).

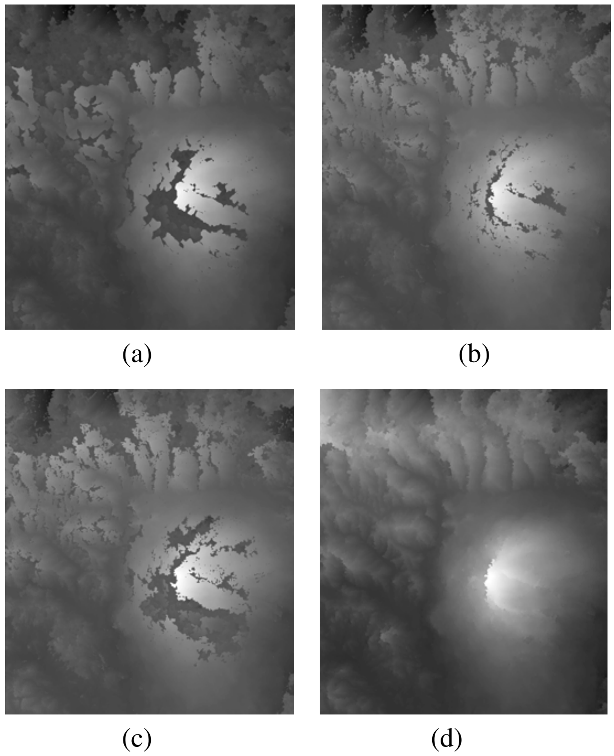

Figure 8. The unwrapped-phase map of figure 6: (a) the phase map unwrapped by Goldstein's branch cuts algorithm; (b) the phase map unwrapped by the mask cuts algorithm; (c) the phase map unwrapped by the plane-fitting algorithm without quality guidance; (d) the phase map unwrapped by our proposed algorithm.

4. Experimental results

Figure 6 is the wrapped-phase map obtained from the interferometry of two real images taken during the tandem campaign by the ERS-1 SAR and the ERS-2 SAR over the region of Mount Etna volcano, Sicily, Italy (grey level representation, 512 × 578 pixels) [18], which contains strong noise, high phase variation and inconsistent areas probably caused by low coherence, layover or other factors.

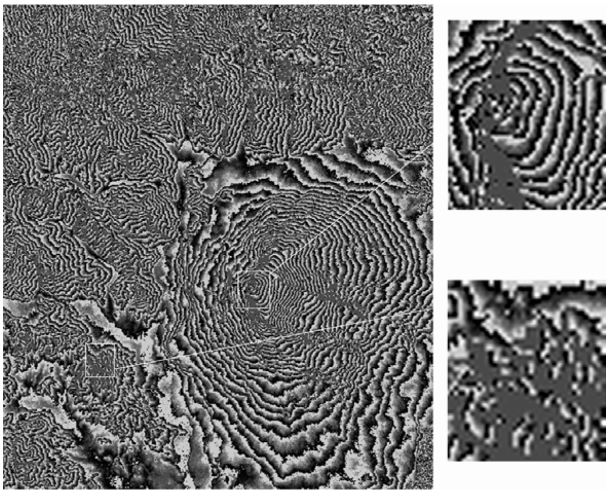

(a)

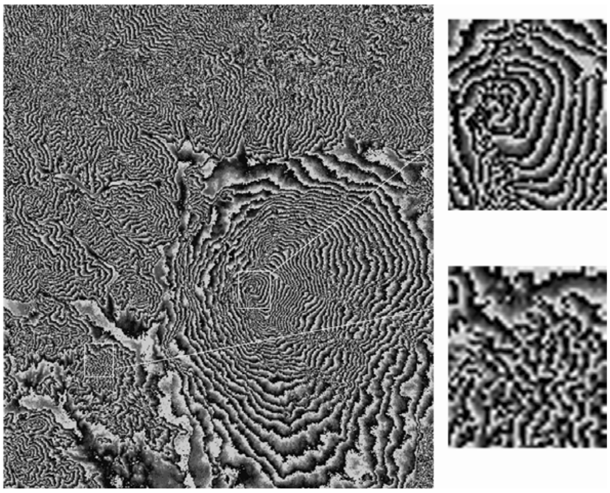

(b)

Figure 9. The rewrapped-phase map (the polluted areas are magnified locally): (a) the rewrapped-phase map of figure 8(b); (b) the rewrapped-phase map of figure 8(d).

Figure 7 is the PDV quality map.

By use of the above four algorithms, we obtain the four unwrapped-phase maps: figure 8(a) is the phase map unwrapped by Goldstein's branch cuts algorithm; figure 8(b) is the phase map unwrapped by the mask cuts algorithm with the PDV quality guidance; figure 8(c) is the phase map unwrapped by the plane-fitting algorithm without quality guidance; figure 8(d) is the phase map unwrapped by our algorithm.

Apparently, there appear some big black spots in figures 8(a)–(c). All the former three algorithms fail to generate correct unwrapped results. In contrast, figure 8(d) shows that our algorithm can produce a reasonable result. In general, rewrapping of the unwrapped maps may be regarded as an efficient method to verify the PhU algorithm [18]. So, for further comparison, we select the least polluted unwrapped-phase maps (figures 8(b) and (d)) and rewrap each of them. The rewrapped-phase maps are shown in figure 9. Figure 9(a) is the rewrapped-phase map of figure 8(b); figure 9(b) is the rewrapped-phase map of figure 8(d).

Figure 9(b) shows that the unwrapped phase obtained by the algorithm proposed in this paper is almost identical to the original wrapped phase (figure 6) when rewrapped. However, figure 9(a) indicates that many areas are corrupted by black stains (we here select two areas to be magnified locally). This unwrapped phase obtained by the mask cuts algorithm is significantly different from the original wrapped phase when rewrapped. Thus it can be seen that our algorithm has an obvious advantage in handling the inconsistent phase map.

The execution time of the proposed algorithm depends on the size of image and particular phase distribution. The tested images are 512×578 pixels in size. The proposed algorithm was executed on a PC system with P4 processor (2667 MHz); the memory on this PC is 512 Mb RAM. The average execution time was about 3 s.

5. Conclusions

We have presented a fast and relatively reliable two-dimensional PhU algorithm. It is based on the simplified plane-fitting assumption for local phase values in the 3×3 window, and the unwrapping process is guided by the PDV quality map. Quality guidance makes sure that the presented algorithm can select the optimal path to perform the unwrapping operation; meanwhile, the local plane approximation provides additional simplification and efficiency in the implementation of the algorithm. The numerical and experimental results have demonstrated that the algorithm proposed in this paper is not only capable of generating a reasonable unwrapped result when strong noise, high phase variation and inconsistencies are present, but also could have higher noise robustness and reliability than the plane-fitting PhU algorithm without quality guidance and the other two conventional path-following algorithms.

References

[1] Schirripa Spagnolo G, Guattari G, Sapia C, Ambrosini D, Paoletti D and Accardo G 2000 Three-dimensional optical profilometry for artwork inspection *J. Opt. A: Pure Appl. Opt.* **2** 353–61

[2] Itoh K 1982 Analysis of the phase unwrapping algorithm *Appl. Opt.* **21** 2470

[3] Volkov V V and Zhu Y 2003 Deterministic phase unwrapping in the presence of noise *Opt. Lett.* **28** 2156–8

[4] Baldi A 2001 Two-dimensional phase unwrapping by quad-tree decomposition *Appl. Opt.* **40** 1187–94

[5] Ghiglia D C and Romero L A 1994 Robust two-dimensional weighted and unweighted phase unwrapping that uses fast transforms and iterative methods *J. Opt. Soc. Am.* A **11** 107–17

[6] Hung K M and Yamada T 1998 Phase unwrapping by regions using least-squares approach *Opt. Eng.* **37** 2965–70

[7] Ghiglia D C and Pritt M D 1998 *Two-Dimensional Phase Unwrapping: Theory, Algorithms, and Software* (New York: Wiley)

[8] Herráez M A, Burton D R, Lalor M J and Gdeisat M A 2002 Fast two-dimensional phase-unwrapping algorithm based on sorting by reliability following a noncontinuous path *Appl. Opt.* **41** 7437–44

[9] Baldi A 2003 Phase unwrapping by region growing *Appl. Opt.* **42** 2498–505

[10] Xu W and Cumming I 1996 A region growing algorithm for InSAR phase unwrapping *Proc. Int. Geosci. Remote Sensing Symp.* pp 2044–6

[11] Goldstein R M, Zebker H A and Werner C L 1988 Satellite radar interferometry: two-dimensional phase unwrapping *Radio Sci.* **23** 713–20

[12] Baldi A, Bertolino F and Ginesu F 2002 On the performance of some unwrapping algorithms *Opt. Lasers Eng.* **37** 313–30

[13] Flynn T J 1996 Consistent 2-D phase unwrapping guided by a quality map *Proc. 1996 Int. Geoscience and Remote Sensing Symp. (Lincoln, NE)* (Piscataway, NJ: IEEE) pp 2057–9

[14] Li W S and Su X Y 2002 Phase unwrapping algorithm based on phase fitting reliability in structured light projection *Opt. Eng.* **41** 1365–72

[15] Lim H, Xu W and Huang X J 1995 Two new practical methods for phase unwrapping *Proc. IGARSS'95 (Firenze, Italy)* pp 196–8

[16] Servin M, Marroquin J L, Malacara D and Cuevas F J 1998 Phase unwrapping with a regularized phase-tracking system *Appl. Opt.* **37** 1917–23

[17] Rivera M and Marroquin J L 2004 Half-quadratic cost functions for phase unwrapping *Opt. Lett.* **29** 504–6

[18] Costantini M 1998 A novel phase unwrapping method based on network programming *IEEE Trans. Geosci. Remote Sens.* **36** 813–21